Available online at www.sciencedirect.com

ScienceDirect

Procedia Manufacturing 47 (2020) 578–585

Procedia MANUFACTURING

www.elsevier.com/locate/procedia

23rd International Conference on Material Forming (ESAFORM 2020)

An Industrial-Scale Cold Forming Process Highly Sensitive to Temperature Induced Frictional Start-up Effects to Validate a Physical Based Friction Model

Mark Veldhuis[a,*], Jörg Heingärtner[b], Anouar Krairi[c], Daan Waanders[d], Javad Hazrati[e]

[a] *Philips, High Tech Campus 5, 5656AE, Eindhoven, The Netherlands*
[b] *Inspire AG, Technoparkstrasse 1, 8005 Zurich, Switzerland*
[c] *Materials innovation institute (M2i), Van der Burghweg 1, 2628 CS DELFT, The Netherlands*
[d] *TriboForm Engineering B.V., Hengelosestraat 500, 7500 AM Enschede, The Netherlands*
[e] *Nonlinear Solid Mechanics, Faculty of Engineering Technology, University of Twente,Enschede, The Netherlands*

* Corresponding author. *E-mail address:* mark.veldhuis@philips.com

Abstract

It is widely realized in the metal forming industry that the processes suffer from start-up effects, which can cause products that fall out of their specification limits after a certain period of running. Attempts are made to solve this by modelling the underlying tribological phenomena in order to design robust processes. Another possibility is to adapt the processes to changes of the tribological system through control systems. For both approaches the ability to account for tribological effects in numerical simulations is a crucial requirement. To showcase this, a real-life demonstrator process is built, that is specifically designed to be sensitive to temperature induced frictional effects. This enables the validation of the physical based tribological models on an industrial scale, without the need to add complexity from other research domains in the field of metal forming. After designing the tooling, the process' sensitivity to temperature induced frictional effects is verified by implementing and applying all simulations tools created [1]. The industrial scale demonstrator process is ran, while measuring tool temperature and geometrical product parameters (quality features) in real-time, at different stroke rates until a steady-state temperature is reached. The recorded data sets, combined with the products themselves, show during the full validation that the predictions from the simulations are generally in good agreement with the results from production.

Keywords: Deep drawing; Friction; Temperature; Start-up effects; Industrial scale demonstrator

1. Introduction

The production stability in the metal forming industry often suffers from start-up effects. This could be improved by model-based prediction and control of temperature-induced friction increase, which is the main topic of the Interreg North West Europe (NWE) funded project Aspect. By capturing the effect of temperature on the total metal forming process and compensate for the rising temperatures during start-up via a control system, this can be reached. This requires models are in place to describe the effect of temperature on the mechanical properties of the steel as well as its effect on friction, both within FEM simulations.

To validate the success of this approach, a specific demonstrator process will be developed. In order to include transient temperature effects and their effect via friction on the forming process, the demonstrator product should be:

10.1016/j.promfg.2020.04.176

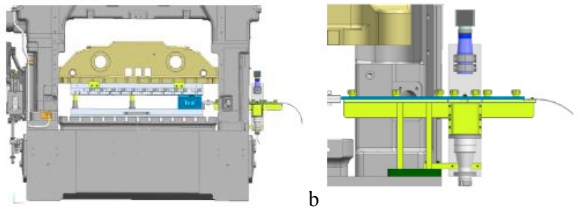

a b

Fig. 1: Press layout (a) for the Aspect demonstrator process together with the vision system to measure the quality (b)

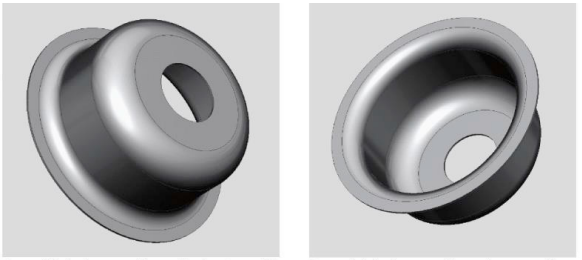

Fig. 2: A deep drawn cup with a hole in the middle, serving as starting idea for the process demonstrator

- Highly influenced by friction
- Generate a great amount of heat via applied work, like in deep drawing
- Preferably not influenced by other potential spread factors, like the flow stress, material thickness or normal anisotropy
- Produce able in a continuous sequence at minimal 60 strokes per minute to generate real start-up effects like in a regular production forming process.

Furthermore, should the resulting and dependent CTQs (Critical To Quality measures) be measurable by a vision system behind the press with sufficient variation in the CTQ-value to be able to distinguish the effect of Temperature on friction and eventually on the product quality. Fig. 1 shows the set-up of the demonstrator process on the Bruderer BSTA 510-125 press with the inline contour measurement connected to it. The test press is well capable of running with a continuous flow as long as the product is produced while being connected to a transportation strip via connectors. The general first idea for a shape that would suit these purposes is a deep drawn cup with a center hole as shown in Fig. 2.

The first design of the process will be fully based on FEM-simulations. Variation analyses will be used to create the optimal process fitting the goals and boundary conditions discussed above. Chapter 2 will elaborate more on the approach taken and will give more details about specific method chosen. The third chapter will show the results leading to the finalized process design. This final process will be simulated using the outputs from [1], including the final friction numbers as a function of the local strain, pressure, sliding velocity and temperature. To verify the temperature-dependence of the process, the tool-temperature will be varied in FEM in the fourth chapter. Chapter 5 will discuss the industrialization of the process and discuss the generated data. The validation of the FEM simulations on product geometry level will be treated in Chapter 6. Finally, in Chapter 7, the conclusions will be drawn and combined with recommendations for future work.

2. Method used for Process Design

In the first design of the demonstrator process, FEM calculations will be used within a DACE approach [2]. In this approach, several noise parameters will be varied, as well as some control parameters to be able to tune the process. Difference with regular robust optimization is however, that variation in the different CTQs does not need to be minimized. The influence of friction shall be maximized, while minimizing the influence of all other (potential) noise parameters. This asks for a slightly different approach, which will be explained in this chapter.

2.1. Noise and control parameters

A set of noise parameters, known for their influence on the forming processes [2], is used for this process design. The variation ranges are tailored to the short-term nature of the process runs, only up-to steady state. An overview of the noise parameters and the variation ranges is shown in Table 1. The normal anisotropy is implemented via a Hill'48 yield criterium, using $R_0 = R_{45} = R_{90} = \bar{R} = x \pm 0.05$. The nominal state is a 0.3mm thick AISI420 in annealed state. The friction is assumed to vary between 0.12 and 0.16 because of temperature fluctuation, based on [3]. Within the simulations, the friction is however varied between 0.1 and 0.2 to ensure a well-fitting metamodel (linked to step 5 in Fig. 5).

The control parameters tool fillet radii, drawing depths and ejector and blank holder forces, as is shown schematically in Fig. 3.

Table 1: Overview of noise parameters and their variation ranges

Parameter	Range
Material thickness (t)	±10 µm
Yield stress (σ_y)	±20 MPa
Friction (μ)	0.12 to 0.16
Normal anisotropy ($\bar{R}$)	±0.05

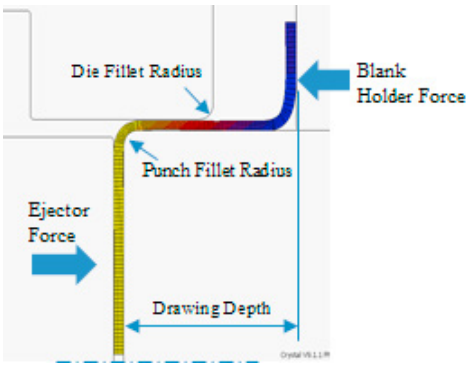

Fig. 3: Schematic overview of varied control parameters in the DACE studies

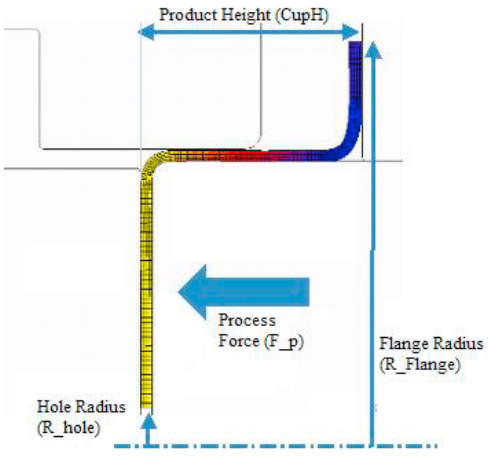

Fig. 4: schematic overview of output parameters (CTQs)

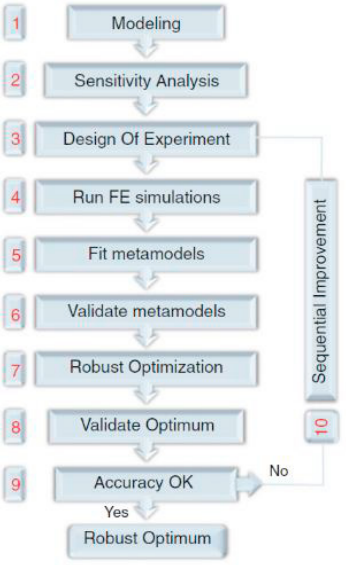

Fig. 5: General DACE approach for robust optimization of processes [2]

2.2. Output parameters (CTQs)

The advantage of a demonstrator process is that the CTQs are not known upfront, so any easy to measure parameters can be used as one. With the camera attached to the press, any profile from a top view of the deep drawn cup can be captured and converted to CTQ-values. Therefore, the hole and flange radius of the cup are logical CTQs and will measured as such from the simulation output.

Other parameters that could be measured within the empirical process later on, are the cup height (also via vision, but then from the side) and the drawing force (by a force sensor attached to the punch). Also, these parameters will be taken from the simulations results.

A schematic overview of all four potential CTQs is given in Fig. 4.

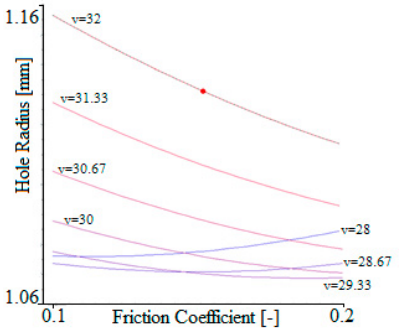

Fig. 6: Graphical representation of an interaction term of a noise (friction) and control parameter (ReDrawVelocity, v) on the value of a CTQ

2.3. Approach to get a friction depended process

As said above, the generally used Design and Analysis of Computer Experiment (DACE) approach is not viable for the demonstrator process, because of goal to make it friction and temperature dependent. The start is very much comparable: steps 1 until 6 are followed as stated in Fig. 5.

The robust optimization now of course cannot happen, since it would mean that the process will also become insensitive to any variation in temperature induced friction variation. Therefore, the process in manually tuned in either tolerance designer or Compact (both software tools created by CQM). The fit of the metamodels is performed in Compact, although it is also possible to do this in MATLAB or Python. When the metamodels are validated, they can be used to graphically show the interactions of various noise parameters and control parameters on one single CTQ. Any term where the value of a noise parameter is multiplied by the value of a control parameter, or higher order multiplication hereof, means that the influence of that specific noise parameter can be tuned by that control parameter. A graphical representation of such an interaction can be seen in Fig. 6. In the figure, one can see the value of CTQ hole radius as a function of the noise parameter friction. The various graphs show this function for a certain value of the drawing depth. For low values of the drawing depth, the variation in hole radius due to friction is not that high. If the drawing depth is increased however, the influence of friction becomes higher. The latter situation is desired for the process design at hand. By tuning the various control parameters using the graphs as presented in Fig. 6, one can increase the influence of friction on the various CTQs, while minimizing the influence of other noise parameters. After optimizing the values of the control parameters, all the metamodels and the values of the different input parameters can be exported to Tolerance Designer. By selecting the appropriate input noise distribution, the expected distribution of the CTQs will be predicted based on a Monte Carlo Analysis using the transfer functions. Furthermore, it can derive what the relative impact of the various noise parameters is on the CTQs. Examples of the predicted CTQ distributions and the relative impact of the noise parameters hereon can be seen in Fig. 7 and Table 2 respectively (numbers are fictive).

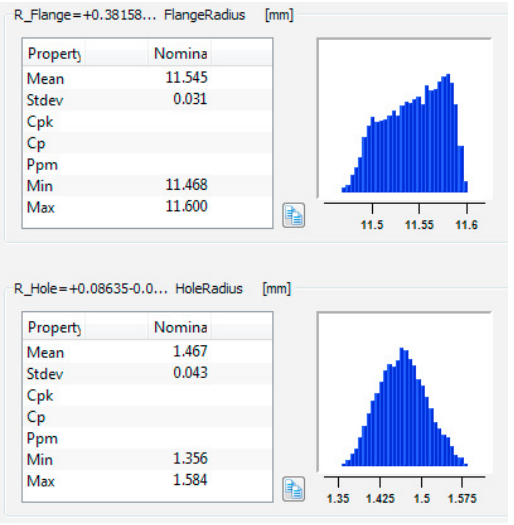

Fig. 7: Typical CTQ-distributions as a result of the MCA in Tolerance Designer

Table 2: Example of the calculated relative influence of the various noise parameters for all CTQs

	CupH	F_p	R_Flange	R_Hole
$\bar{R}$	64%	1%	98%	46%
μ	13%	74%	1%	48%
σ_y	35%	24%	2%	4%

In this research, uniform distributions are selected, since it gives a worst-case scenario and due to the short nature of the production runs, the full normally distributed variation window is often not addressed.

Looking at the predicted distribution for the CTQs, one can decide if the variation is large enough to be measured in a robust way by the vision system behind the press. The vision system is expected to be able to measure diameters like the hole and flange diameter robustly for variations in the order of 1 micron.

3. Process designs and results

As stated in Chapter 1, deep drawing is one of the metal forming processes where the most heat is generated. Steady state temperatures in deep drawing processes can easily rise to 80°C [4], giving a clear start-up effect when starting from room temperature. This makes a deep drawing process an ideal process to be investigated. The specific execution is to be tuned to give a maximum impact of friction on the output CTQs only, so limited or no influence of other noise parameters on these CTQs. Various types of deep drawing processes are investigated to see how they are behaving with respect to this goal. For all these processes, various control parameters are varied as already stated in Section 2.1, but the following general deep drawing processes can be identified:

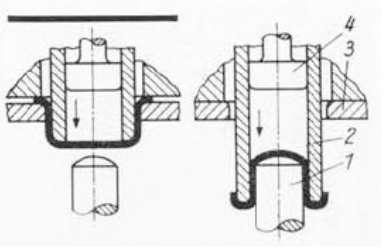

Fig. 8: Schematic representation of a two-step redrawing process [5]

- Simple deep drawing of a cup: so, with a rather small punch fillet radius and a large die fillet radius. The drawing ratio is safely within the limits of the material.
- Deep drawing with a very large punch fillet radius. Drawing ratio is in the same order as for process 1.
- Two-step redrawing: First a simple deep drawing as in process 1 is executed and afterwards a second step in the opposite direction, where cup radius is reduced. This is schematically shown in Fig. 8.

3.1. Results per process

The simple deep drawing process showed to be relatively insensitive to friction, compared to the other potential noise factors.

The deep drawing process with large punch fillet radius seemed to work, but only in the case that the bottom side is not flat, which would lead to an unwanted shadow effect in measuring the hole radius, which would lead to spread on this measurement. As the CTQ is already changing due to changing start-up conditions, the need of averaging to overcome measurement noise is highly unwanted. Attempts to overcome this, resulted in the same outcome as for the first process (see Appendix A. for more details).

The third process option showed the most promising results, especially after adding a blank holder in the redrawing step. For the hole radius, the influence of the other noise parameters remains limited, whilst the influence of friction shows to be the dominant factor, as can be seen in Table 3. On top of that, the hole radius shows a variation window of about 0.03mm (see Fig. 9) which seems traceable in a robust way with the desired camera system.

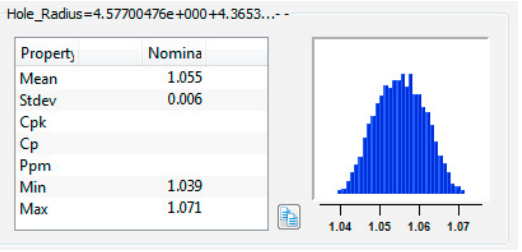

Fig. 9: CTQ-distribution as a result of the MCA in Tolerance Designer for the two-step redrawing process with blank holder

Table 3: Relative impact of the noise parameters as a result of the MCA in Tolerance Designer for the two-step redrawing process

	CupH	R_Flange	R_Hole	F_p
σ_y	2%	0%	-	3%
μ	-	30%	69%	1%
$\bar{R}$	0%	44%	10%	1%
t	98%	24%	19%	96%

3.2. The final process

The final process for the demonstration-line, as designed on the above DACE studies consists of four dies in a specially designed die housing, as shown in Fig. 10. The process consists of (full details are added in Appendix B.):

- Die 1: Cutting out positioning holes, used to correctly position the strip in the succeeding process steps, together with the product center hole.
- Die 2: Cutting free the blank shape
- Die 3: Deep drawing step
- Die 4: Re-drawing step

The products created by the different die sets are visualized in Fig. 11. The cutting of the center hole and the flange diameter by dedicated cutters will keep starting variation in sub-micron level.

In die 3 and 4, thermocouples are placed, to be able to measure the (local) temperature in the tools, as shown in Fig. 12. In this way, the temperature during start-up can be measured and linked to local friction effects later on.

The tool has the option to place a force sensor on top of the punch of the second step, but the implementation is pending at the moment of writing.

In the die housing, four lever systems are placed that can be actuated by their individual motors (see Fig. 13). In that way the Blank holder and Ejector forces can be adjusted in both steps, such that normal forces and consequently contact pressures can be changed. At the same time, this option will be used by separately designed control system, discussed in [6].

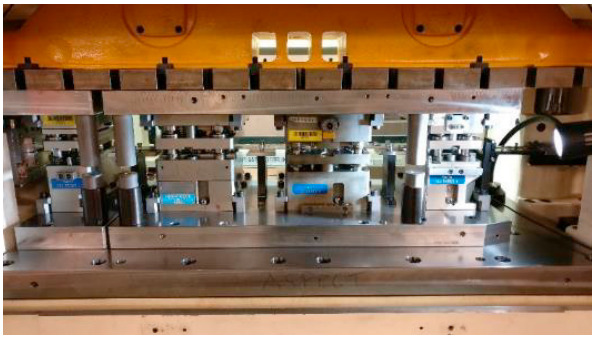

Fig. 10: Tooling for an Industrial-Scale Cold Forming Process Highly Sensitive To Temperature Induced Frictional Start-up Effects, consisting of 4 succeeding dies (named die 1 till 4 from left to right).

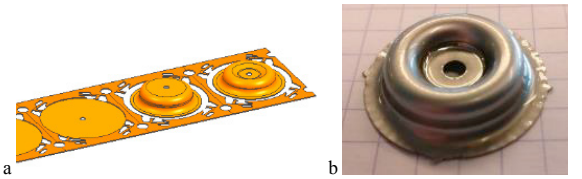

Fig. 11: The strip layout of the demonstrator process (a) and its empirical end result (b).

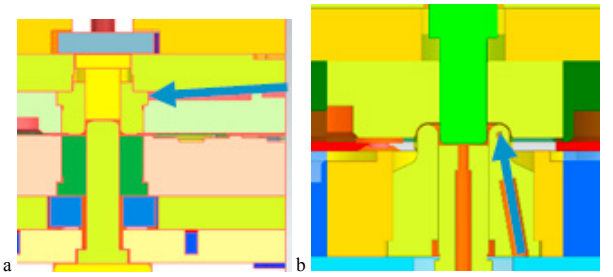

Fig. 12: Thermocouples, indicated by the blue arrows, in the tool to measure (local) tool temperatures during start-up: a) at the outside of the die bush in the die 3 (deep drawing step); b) near the fillet radius of the die in die 4 (redrawing step)

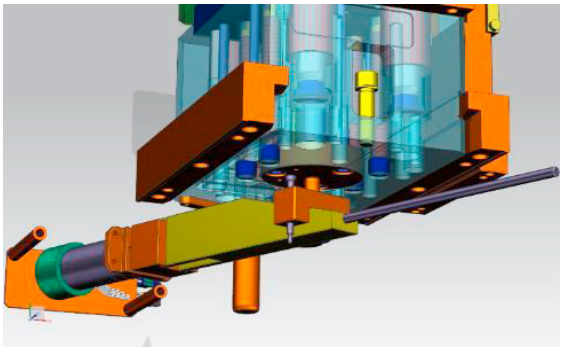

Fig. 13: Motor driving the leaver system to set the pretension of the ejector and blank holder

4. Verification

To verify if the process, as developed in Chapter 3, shows high dependency on temperature-induced frictional effects, the simulation of the process is extended to a version with meshed tools, such that the temperature distribution in the tools can be captured. The axisymmetric MSC.Marc simulation also uses the user subroutine developed within the Aspect project. In this user subroutine, temperature depended strain hardening is incorporated via the routine WKSLP. In WKSLP, the modified Bergström model is implemented, as proposed in [1]. Furthermore, the temperature dependent friction model, as developed in [7], is included in the user subroutine. For every node in contact, the in-plane plastic strain, contact normal pressure, sliding velocity and temperature of the product are determined. These four parameters serve as an input for a 4D table, from which the corresponding friction coefficient is determined. The locally determined nodal friction coefficient is subsequently used in the next increment.

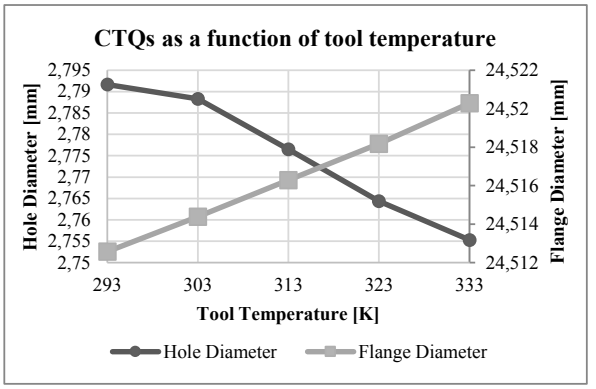

Fig. 14: The hole and flange radius as a function of temperature using the Aspect user subroutine

Varying the tool temperature in the simulations serves as an indicator how the process will react to heating up of the tool during process start-up in practice. The results are shown in Fig. 14. The variation in hole diameter shows a decreasing trend with tool temperature, as a consequence of the higher friction values at higher temperatures. The change in flange diameter shows an opposite trend, but the total variation stays limited to 0.01mm over the full temperature window, whereas the variation in hole diameter shows triple this variation.

5. Empirical results and trend validation

The designed process is tested in practice, keeping track of tool temperature, using the thermocouples installed according to Fig. 12, and the camera system, already shown in Fig. 1, measuring hole and flange diameter. For clarity, the temperatures are shown in Fig. 15 and Fig. 16 in the same manner. The measured CTQs hole and flange diameter are shown in Fig. 15 and Fig. 16 respectively.

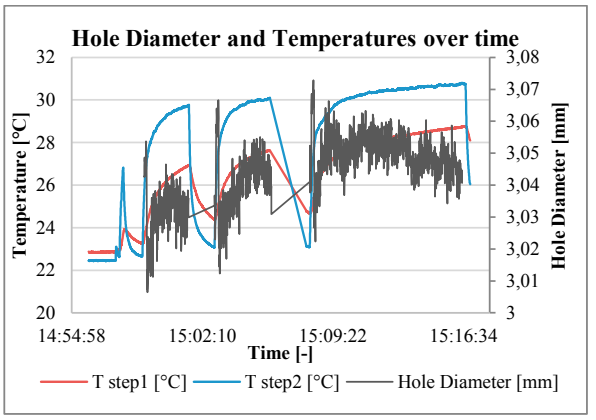

Fig. 15: Empirical results for Temperature and Hole diameter measurements over time

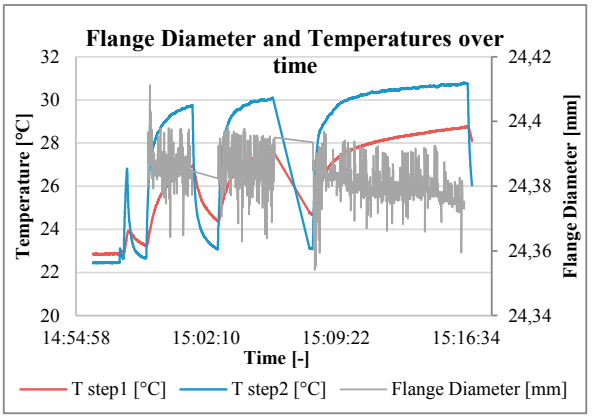

Fig. 16: Empirical results for Temperature and Flange diameter measurements over time

In the figures, it can be seen that the temperature rises quickly when production is started, but also rapidly drops when production stops. The tests done at the moment of writing are not perfect yet, meaning that steady-state could not be reached before the production is automatically stopped due to a strip positioning error (small ones in the stops in the graph, more severe one at the end). This also means that the full temperature window from Fig. 14 has not been tested yet, which is thought to be reached after ~1 hour with tool temperatures up to 50°C. However, from the results it can be seen that indeed the temperature is rising quickly during start-up and both the flange and hole diameter are changing as well, meaning that start-up effects are visible and the designed process meets its initial targets.

Looking at the lines for the hole and flange diameter now, it can be seen that quite some short-term variation is present, which is thought to be measurement spread. When looking at the trends, it can be seen that the flange diameter is reducing slightly with time and temperature. For the hole diameter, the trend seems to be twofold. In the first part, lasting about 2 minutes, the diameter increases and from that point onwards a decreasing trend can be observed. That latter part is expected from the simulations as a function of temperature. The increase in the first part means that the friction is reducing. Current hypothesis is that a dynamic film layer of lubricant is building up over time and only when this layer has reached a stable thickness, the temperature effect becomes more pronounced. This should be confirmed by longer test runs in the future.

6. Product geometry validation

In this Chapter, the product shape from the simulations discussed in Chapter 4 is compared to the shape of a product created in practice. This is done for a product, created with cold tools. This product is analyzed via an X-ray measurement first. The measurement results are shown in Fig. 17 and indicated that a cross section can be made best along the x-axis, which coincides with the rolling direction of the strip.

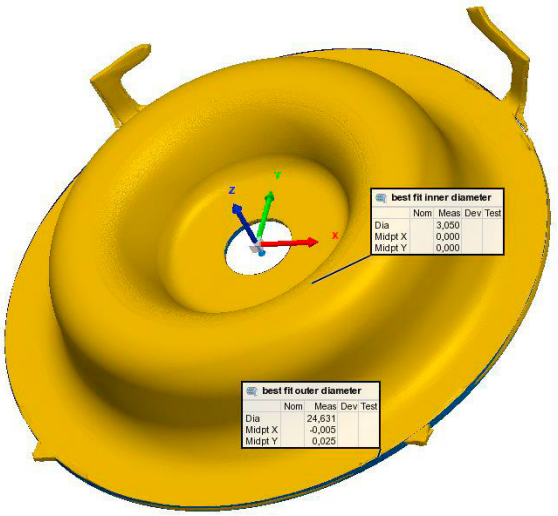

Fig. 17: X-ray measurement of an Aspect product with fitted circles for flange (d=24.631mm) and hole diameter (d=3.05mm), showing the flange to be 5µm eccentric along the x- and 25µm eccentric along the y-axis

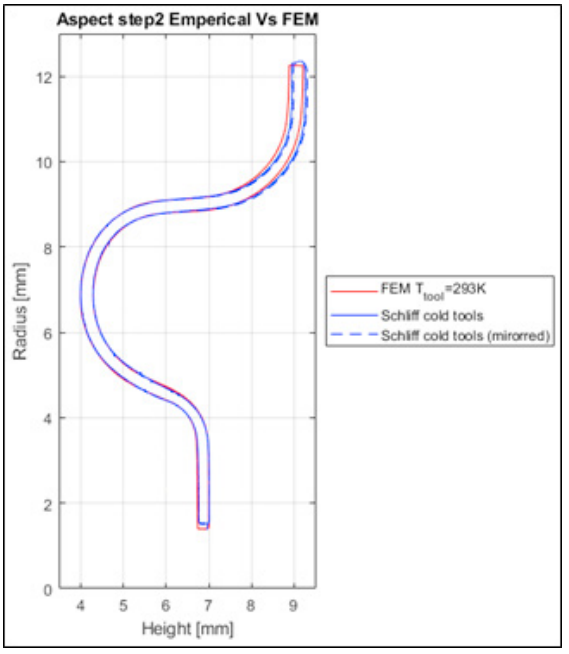

Fig. 18: FEM result plotted over a cross section measurement (and a mirrored version of that)

Based on this X-ray measurement, the same product is embedded in an epoxy, after which it is grinded in half gradually, to create a near perfect cross section (schliff). This cross section is measured using image analysis. The measurement results are plotted on top of the product cross section from the FEM simulations, as can be seen in Fig. 18.

Comparing the results from the FEM simulation to the measurement of the schliff, one can see a rather good agreement, apart from the product height. This can specifically be observed by the mismatch along the x-axis in the flange area. Current hypothesis is that this difference is caused by the small wrinkles that are present in the flange in practice (initiated in the deep drawing step), which is not covered by the FEM simulations. This results in a relatively stiffer flange in practice, which is therefore pulled in less during redrawing, resulting in a relatively higher product. At the same time, if less material is pulled in from the flange area, the hole diameter will increase more, which is in agreement with the differences seen in that area.

7. Conclusions and recommendations

The cold forming process designed in this paper has shown to meet its targets on generating heat via applied work and geometrical product measures that change during start-up, which can be measured adequately by a camera system. This means that the process fits its purpose of validating a temperature dependent friction model extremely well.

The validation of that temperature dependent friction model shows in general satisfying results. Some differences are still present in the very first part after production start, which is thought to be caused by the built up of a dynamic layer of lubricant. After this phase, the trend as a function of temperature shows rather good agreement with trends predicted by the FEM model with temperature dependent friction values.

On product level also some differences are still observed, which is probably caused by the presence of wrinkles in the flange in practice, which cannot be captured in the asymmetrical FEM simulations.

To be conclusive on these posted hypotheses, it is recommended to solve the errors in production, to be able to do runs to steady-state value of the tool temperature. In that way, the trends of the full temperature window can be captured in a more accurate manner. Furthermore, it is recommended to solve the wrinkling in practice, to come to matching flange stiffness in practice and the FEM simulations.

Acknowledgements

This research was carried out within the project “ASPECT – Advanced Simulation and control of tribology in metal forming Processes for the North-West European Consumer goods and Transport sectors” (project number NWE 220), co-funded by the INTERREG North West Europe program www.nweurope.eu/aspect

Appendix A. Relative impact of noise parameters and CTQ variation for deep drawing with a large punch fillet radius

The detailed results for deep drawing process with large punch fillet radius are given in Fig. 19 and Table 4. Fig. 19 shows the expected variation window of the hole radius, whereas Table 4 shows the relative impact of the noise parameters. The latter shows that other noise factors are too dominant for this process.

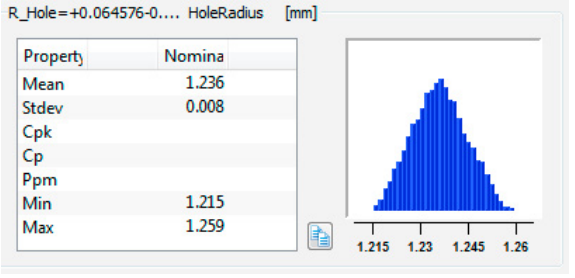

Fig. 19: CTQ-distribution as a result of the MCA in Tolerance Designer for the deep drawing process with large punch fillet radius

Table 4: Relative impact of the noise parameters as a result of the MCA in Tolerance Designer for the deep drawing process with large punch fillet radius

	CupH	R_Flange	R_Hole	F_p
$\bar{R}$	89%	87%	48%	13%
μ	1%	2%	45%	10%
σ_y	11%	13%	7%	78%

Appendix B. Aspect demonstrator Process Details

The process details are:

- Die 1: Cutting out positioning holes, used to correctly position the strip in the succeeding process steps, together with the center hole (2 mm in diameter).
- Die 2: Cutting free the blank shape (diameter of 29.5mm), with local connection to the connector strip with positioning holes
- Die 3: Deep drawing step, with tool specifications:
  - Die: inner diameter of 18.36mm and a fillet radius of 2.0mm
  - Punch: outer diameter of 17.7mm with a fillet radius of 2.00mm
  - Drawing depth: 5.51mm
  - Blank Holder Force:
    - At start: 300N
    - At final depth: 635N
  - Ejector Force:
    - At start: 0N
    - At final depth: 58N
- Die 4: Re-drawing step, with specifications:
  - Die: outer diameter of 17.6mm; inner diameter of 9.6mm and a fillet radius of 2.0mm
  - Punch: outer diameter of 8.94mm with a fillet radius of 1.00mm
  - Drawing depth: 2.74mm
  - Blank Holder Force:
    - At start: 96N
    - At final depth: 328N
  - Ejector Force:
    - At start: 25N
    - At final depth: 53N

References

[1] Wang C, Hazrati J, De Rooij MB, Veldhuis M, Aha B, Georgiou E, Drees D, Van den Boogaard AH, Temperature dependent micromechanics-based friction model for cold stamping processes, Journal of physics: Conference series 2018; 1063: 1-6
[2] Wiebenga, JH, Robust design and optimization of forming processes, PhD thesis, University of Twente, 2014
[3] Grueebler R, Hora P, Temperature Dependent Friction modelling for sheet metal forming, Int J Mater Form 2009; 2(1): 251–254
[4] Pereira, MP and Rolfe, BF, Temperature conditions during 'cold' sheet metal stamping, Journal of Materials Processing Technology 2014. 214 (8): 1749-1758
[5] Romanovski WP, Handboek voor Moderne Stanstechniek. Deventer: Æ. E. Kluwer; 1959
[6] Heingärtner J, Veldhuis M, Kott M, Hora P, Process Control of Forming Processes to Compensate Temperature Induced Friction Changes. 23rd International Conference on Material Forming (ESAFORM 2020)
[7] Waanders D, Hazrati Marangalou J, Hol J, Temperature Dependent Friction Modelling. 23rd International Conference on Material Forming (ESAFORM 2020)